Plasma Processes and Polymers

PLASMA PROCESSES AND POLYMERS

RESEARCH ARTICLE OPEN ACCESS

Effect of Atmospheric Pressure Nonequilibrium Plasma Pretreatment of Polyethylene/Polypropylene on Epoxy Adhesively Bonded Joints

Kosuke Takenaka[1] | Ryosuke Koyari[1] | Shunsho Shigemori[1] | Giichiro Uchida[2] | Yuichi Setsuhara[1]

[1]Joining and Welding Research Institute, The University of Osaka, Ibaraki, Osaka, Japan | [2]Faculty of Science and Technology, Meijo University, Tempaku-ku, Nagoya, Japan

Correspondence: Kosuke Takenaka (takenaka.kosuke.jwri@osaka-u.ac.jp)

Received: 14 May 2025 | **Revised:** 5 August 2025 | **Accepted:** 8 August 2025

Funding: This study was supported in part by funding from DAIHEN Welding and Joining Research Alliance Laboratories at Joining and Welding Research Institute, Osaka University.

Keywords: atmospheric pressure plasma | cold-rolled high tensile strength steel | epoxy adhesive bonding | polyethylene | polypropylene | SPFC980Y

ABSTRACT

Effects of atmospheric-pressure nonequilibrium plasma pretreatment of polyethylene (PE) and polypropylene (PP) on epoxy adhesively bonded joints have been investigated. The atmospheric-pressure plasma sustained by RF power (RF plasma) and high-voltage DC pulses (LF plasma) have been used to pretreat PP and PE surfaces. The tensile shear stress of epoxy-bonded joints between cold-rolled high-tensile-strength steel (SPFC980Y) and PE or PP pretreated with RF and LF plasma exhibited significantly higher values than those of the untreated counterparts. The results for SPFC980Y-PP joints were greater for LF plasma treatment than for RF plasma treatment. The loss in bonding strength observed with RF plasma treatment was attributed to the thermal degradation of PP caused by the heat flux from the plasma.

1 | Introduction

Metal-polymer hybrid materials have the potential to combine the mechanical properties of these two materials, which is key because of the demand for lightweight design, functional integration, and cost reduction. Among the many types of polymers, polyethylene (PE) and polypropylene (PP), known as polyolefins, are the most widely used because of their excellent properties, such as low density, chemical inertness, low-cost versatility, and electrical properties, such as insulation. Therefore, they are widely used as materials for many industrial products, including automobiles, electronics, and biomedical applications [1–6]. The main bonding mechanism in metal-polymer direct bonding or adhesive bonding is a hydrogen bond between the hydroxyl group at the surface of the metal oxide layer and the polar functional group on the surface of the polymer materials. On the other hand, PE and PP are difficult to bond because of their inert structure in the absence of polar functional groups. To make PE and PP bondable, polar functional groups (carboxyl, amino, hydroxyl, etc.) must be added to the PE and PP surfaces via surface modification [7, 8].

Currently, the methods of surface modification for polymer include chemical etching using acids and alkalis [8, 9], UV irradiation [10, 11], and plasma treatment [12]. Although surface modification of PE and PP via acid–alkali etching and ultraviolet irradiation has been explored [13] investigations addressing the bonding strength between these substrates and epoxy adhesives remain exceedingly scarce.

Among these, plasma treatment is advantageous because it selectively modifies only the surface of the polymer materials [12, 14–18]. An atmospheric-pressure RF plasma jet has been proposed as a pretreatment method for polymer surfaces before adhesive bonding.

This plasma jet not only efficiently supplies oxygen radicals through high-density Ar plasma generation and the reaction between the Ar plasma and oxygen in the air blown into the atmosphere, but also facilitates surface reactions of active species due to the heat flux provided by the plasma (gas temperature around 150°C) [19, 20]. Therefore, the application of atmospheric-pressure RF plasma jets enables effective functionalization of metal and plastic surfaces. Furthermore, plasma treatment constitutes an advanced surface modification technology that facilitates the precise and controlled alteration of polymer surfaces while imposing minimal environmental impact.

The direct joining of SUS304 stainless steel and polycarbonate (PC), an engineering plastic with a low glass transition temperature, has been demonstrated by combining surface treatment and heating with an atmospheric-pressure RF plasma jet without an external heating source apart from the plasma itself [21]. In direct metal-polymer bonding, the chemical effects of plasma irradiation have a greater impact on bonding strength than physical effects such as surface morphology has been demonstrated [21]. Furthermore, aluminum alloys A1050 and A5052, pure titanium TP340, and engineering plastic polyetheretherketone (PEEK) were directly joined by hot pressing following surface pretreatment with atmospheric-pressure RF plasma jets, confirming the effect of plasma treatment on bond strength [22–24].

In this study, the epoxy adhesive bonding of cold-rolled high tensile strength steel (SPFC980Y) to PE and PP under pretreatment by an atmospheric-pressure nonequilibrium plasma jet was demonstrated. The differences in the effects of pretreatment with atmospheric-pressure plasma sustained with RF plasma and LF plasma on the adhesive bonding of SPFC980Y-PP and SPFC980Y-PE were investigated, focusing on surface modification of PP and PE with inert structures.

2 | Experimental Procedures

The test pieces of metal used were 500 × 15 × 1.5 mm sheets of cold-rolled high tensile strength steel, SPFC980Y, and the test pieces of thermoplastic were 500 × 15 × 5 mm sheets of PP and PE.

An atmospheric pressure RF plasma jet was produced using two copper sheet strips with lengths of 15 and 5 mm. The two metal strips were wrapped around a quartz tube to serve as the power and ground electrodes, respectively, as schematically shown in Figure 1a. The 5 mm length copper sheet strip as used ground electrode was positioned at the head of the quartz tube, and the 15 mm length copper sheet strip as used power electrode was set 5 mm away from the edge of the ground electrode. The outer and inner diameters of the quartz tube were 6 and 4 mm, respectively. Sine-wave voltages of frequencies 60 MHz were applied to the power electrode. The RF power and the flow rate of Ar gas (purity of 99.999%: Iwatani Fine Gas Co. Ltd.) were fixed at 98 W and 3 slm, respectively [19, 20].

An experiment using an atmospheric pressure LF plasma jet was also performed to establish the effects of using different plasma sources. This LF plasma jet was obtained by wrapping a

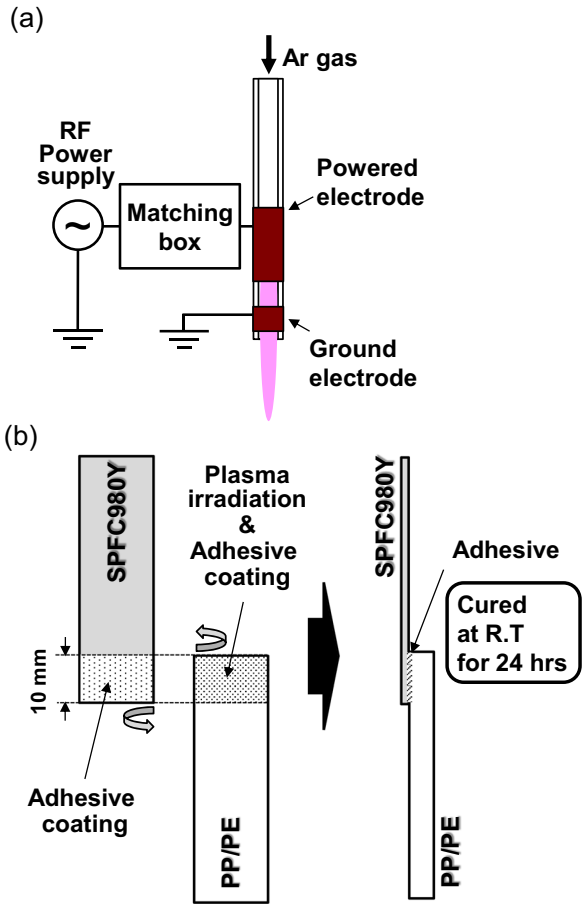

FIGURE 1 | Schematic illustrations of (a) an atmospheric pressure RF plasma jet and (b) bonding procedure of dissimilar metal-organic materials using an atmospheric pressure plasma jet.

quartz tube with 45- and 15-mm-wide copper metal strips serving as the power and ground electrodes, respectively. The power electrode was set at 4 mm from the outlet of the quartz tube, and the distance between the power and ground electrodes was 8 mm. To initiate dielectric barrier discharge between the electrodes within the quartz tube, the power electrodes were connected to a high-voltage pulsed power source, delivering voltage pulses with a peak-to-peak amplitude of 10 kV at a frequency of 5 kHz. A He gas (purity of 99.999%: Iwatani Fine Gas Co. Ltd.) was supplied to the quartz tube as a dischage gas at a flow rate of 3 slm to generate an LF plasma jet [20].

Plasma irradiation was conducted by positioning the samples on an automated stage (Sigma Koki) operating at 40 mm/s, which scanned and treated the entire bonding surface. Each complete scan of the bonding area required 10 s.

The surface temperature of PP and PE surfaces during plasma treatment was measured in situ using an infrared thermometer (MICRO-EPSILON, thermoMETER: 3MH-CF3-CB3).

Figure 1b shows the procedure for adhesive bonding to metal and polymer materials using an atmospheric-pressure RF plasma jet. The PP and PE surfaces were treated with an atmospheric-pressure RF plasma jet as a pretreatment for the bonding process. All samples not subjected to plasma treatment were evaluated in the as-received condition. A commercially

available epoxy adhesive, TB2087 from ThreeBond Co. Ltd., comprising a two-component system consisting of an epoxy resin (Bisphenol A liquid epoxy resin) and a hardening agent (polyamidoamine), was utilized (Tensile shear strength of the epoxy adhesive after curing: 17 MPa). After uniformly mixing equal amounts of epoxy resin and hardening agent including (1:1), a thin adhesive layer was applied to the bonding surfaces of the SPFC980Y-PP and SPFC980Y-PE. The metal and polymer were bonded with an overlap of 10 mm, and the assembly was fixed and cured at room temperature for 24 h, as shown in Figure 1b.

A tensile shear test of the adhesively bonded joints was performed to determine joint strength. A tensile tester was used for the tensile shear tests (Autograph AGS-X: Simatzu Corporation). The load axis was adjusted to coincide with the center of the bonded surface so that the shear force was applied to the bonded interface. The metal side and polymer side were clamped parallel to the tensile axis, and the crosshead speed was 1.66×10^{-3} mm/s. The maximum load at break was measured for each joint formed under different conditions.

The surface morphologies of PP and PE were examined using atomic force spectroscopy (AFM) (KEYENCE VN-8000). All AFM images in this study were acquired from $10 \times 10\,\mu m$ regions. The hardness of the PP and PE surface layers was measured using a micro-Vickers hardness tester (Mitutoyo, HM-221). The diagonal length of each indent, d (mm), was measured using optical microscopy, then converted to Vickers hardness, HV (N (kgf)/mm^2), using the following equation [25]

$$\mathrm{HV} = 1.854\frac{F}{d^2}, \tag{1}$$

where F (N (kgf)) is the indent load ($F = 0.98$ N (100 gf) in this study). The Vickers hardness measurements were evaluated as the average of multiple measurements.

3 | Results and Discussion

To investigate the influence of plasma treatment on PE and PP surfaces on the epoxy adhesively bonded joints, the epoxy adhesively bonded joints of SPFC980Y bonded to PE and PP pretreated with RF and LF plasma were fabricated, and the bond strength of the joints was evaluated.

Figure 2 shows the tensile shear strength of the epoxy adhesively bonded joints of SPFC980Y bonded to PE and PP pretreated with RF and LF plasma, together with that of the untreated PE and PP. In the bonding of SPFC980Y to PE, the joint prepared with untreated PE exhibited a tensile shear strength of 1.0 MPa. In contrast, the joint using LF plasma-treated PE exhibited a strength of 5.1 MPa, approximately 5.1 times higher than that of the untreated sample. The joint bonded with RF plasma-treated PE showed a similar strength of 6.2 MPa, comparable to that of the LF plasma-treated joint. In the bonding of SPFC980Y to PP, the joint with untreated PP exhibited a tensile shear strength of 0.6 MPa. The adhesive joint using LF plasma-treated PP exhibited a strength of 6.1 MPa, approximately 10 times higher than that of the untreated sample. In contrast, the adhesive joint prepared with RF plasma-treated PP showed a lower strength of 3.4 MPa compared to the LF plasma-treated joint. Figure 3 shows photographs of the fracture surfaces after tensile testing of joints adhesively bonded to PP and PE substrates treated with either LF or RF plasma. In all joints, interfacial failure occurred on the polymer side, with the adhesive remaining on the metal surface. The visual inspection of the polymer side revealed no observable epoxy adhesive residues or evidence of material delamination. Epoxy resins are generally known for their strong adhesion to metals. This high adhesive strength is attributed to the formation of strong hydrogen bonds between hydroxyl groups in the epoxy resin monolayer and water molecules adsorbed on the metal surface [26]. In addition, the epoxy adhesive used in this study employs polyamideamine as a curing agent, which introduces amino groups into the cured resin. The strong adhesion observed is likely due to interactions between the N^+ derived from the polyamideamine and the hydroxyl groups present on the metal surface [27].

To study the cause of variation in bond strength of the bonded sample plasma-treated samples, the effect of plasma irradiation on the physical and chemical state of the metal/polymer surface was investigated.

The chemical state of the surface of the PE and PP after irradiation with both plasmas was analyzed using XPS. Figure 4

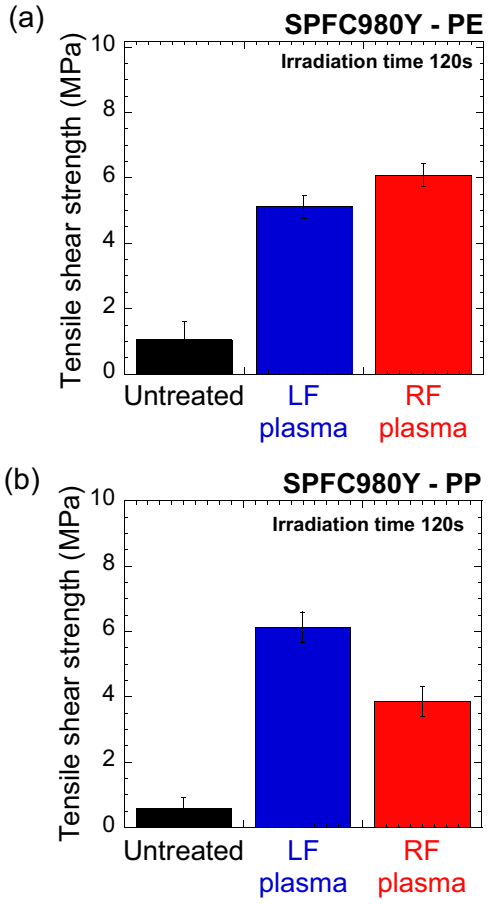

FIGURE 2 | Tensile shear strength of SPFC980Y-PE/PP adhesive bonding samples utilizing (a) RF and (b) LF plasma-treated PE/PP, along with that of untreated PE/PP.

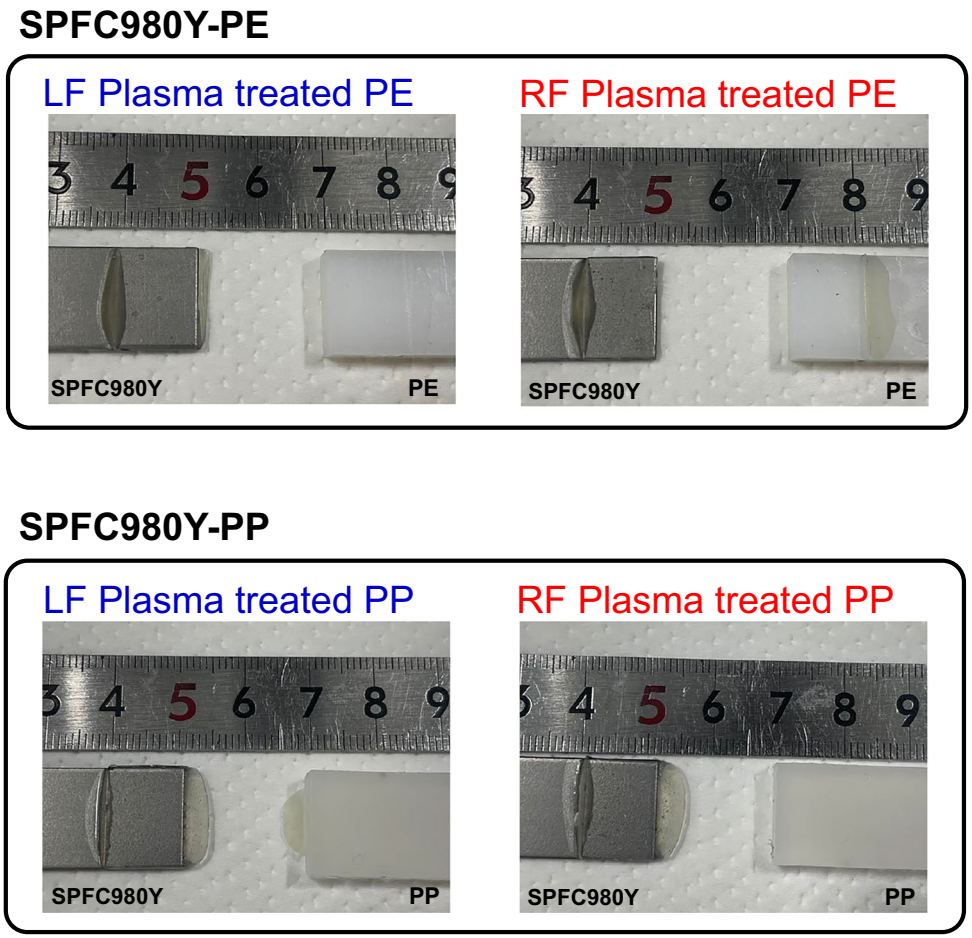

FIGURE 3 | Photographic images of fracture surfaces after tensile testing of specimens bonded to PP and PE substrates treated with LF and RF plasma irradiation.

shows the XPS C 1 s spectra of the untreated PE and PP surface and the PE and PP surface subjected to LF and RF plasma irradiation for 120 s. The C1s spectrum of untreated PP and PE film contained peak at 285.0 eV, corresponding to C–C [28]. The spectra of LF plasma-treated PE and PP surface also showed peaks for C–C additional peaks at 286.5 and 287.7 eV also arise which may be due to C–O and C=O [28]. The presence of an O=C peak in the chemical structure on the PE and PP surface indicates formation by the irradiation of oxygen radicals resulting from the oxidation of the plasma jet. In addition, the XPS C1s spectra of both PP and PE subjected to RF plasma treatment exhibited a distinct peak at 289.1 eV, which is attributed to O–C=O [28]. It is generally known that in the joining of dissimilar materials, bonding occurs through hydrogen bonding involving polar functional groups such as O=C–O and C=O, as well as hydroxyl groups [29–31]. The XPS results suggest that the introduction of functional groups onto the surfaces of PE and PP contributes to enhanced interfacial adhesion strength. Figure 5 shows the ratio of the total area of C–O, C=O, and O–C=O bond peaks to the C–C bond peak area calculated from the XPS C1s spectrum. In both results for PP and PE, the O/C ratio obtained by XPS analysis was higher following RF plasma treatment compared to LF plasma treatment. These results can be attributed to the substantially higher density of oxygen radicals generated by RF plasma sources relative to LF plasma sources, as well as the thermal energy input during plasma exposure, which leads to a rise in surface temperature. These conditions are considered to promote more effective oxidation of the polymer surfaces under RF plasma treatment. The amount of oxygen incorporated on the surface was greater for PP than for PE, a tendency that was particularly pronounced under RF plasma treatment. The correlation between bond strength and oxygen functionalization induced by RF and LF plasma treatments revealed no significant variation in bond strength, implying that factors beyond chemical modification may contribute to the adhesion mechanism.

To investigate the influence of the physical properties of PP and PE on their joint strength, the surface morphology of both materials was examined. The roughness of the PE and PP surface after irradiation with both plasmas was analyzed using AFM. Figure 6 shows the R_a of the (a) PE and (b) PP surfaces as a function of plasma irradiation time. In LF plasma irradiation, the surface roughness of both PE and PP remained nearly unchanged, even with an increase in irradiation time. In contrast, in RF plasma irradiation, the surface roughness increased significantly after 120 s of plasma exposure and was substantially greater than that observed in LF plasma irradiation. In general, it is known that the surface roughness correlates with the bonding strength. However, in this experiment, while the surface roughness increased with RF plasma irradiation compared to LF plasma irradiation, no effect on bonding strength

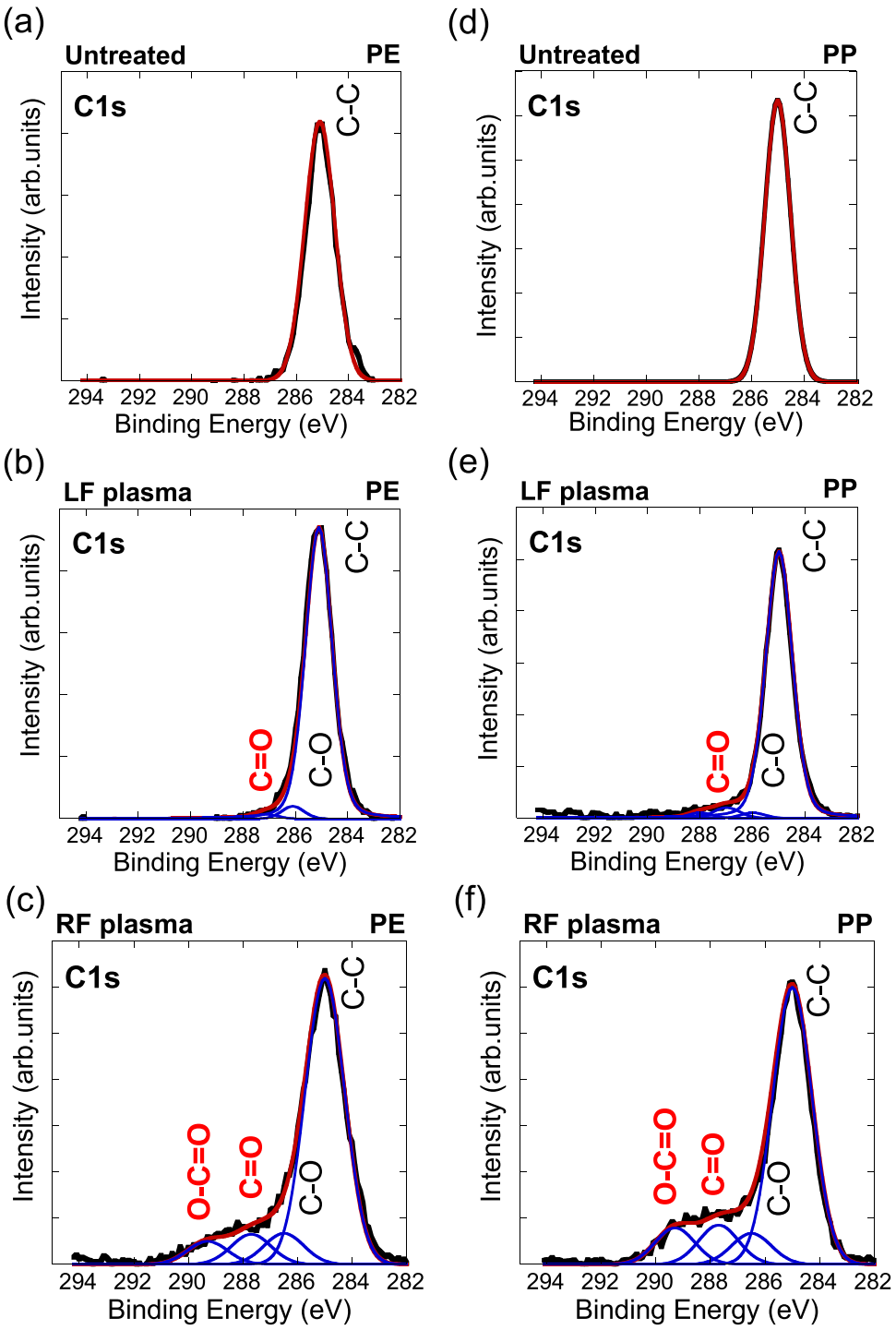

FIGURE 4 | XPS C 1 s spectra on surface of (a) untreated PE, (b) LF plasma-irradiated PE, (c) RF plasma-irradiated PE, (d) untreated PP, (e) LF plasma-irradiated PP, and (f) RF plasma-irradiated PP.

was observed, suggesting that the effect of surface roughness on bonding strength was small.

Accordingly, this study focused on the surface hardness of PE and PP as another physical factor affecting joint strength. The surface hardness of PP and PE was evaluated using the Vickers hardness test. Figure 7 shows the variation in the Vickers hardness with plasma irradiation as a parameter of the plasma irradiation condition. The Vickers hardness of PE surface remained nearly constant regardless of the type of plasma applied or the irradiation time. In contrast, the Vickers hardness of the PP surface exhibited minimal variation under LF plasma irradiation, whereas a progressive decline of the Vickers hardness was observed with increasing irradiation time under RF plasma exposure. To investigate the effect of heat on the Vickers hardness of PP during the plasma irradiation process, with a focus on thermal input from RF plasma, the Vickers hardness of the PP surface was measured after heating with a heater at different temperatures. Figure 8 shows the substrate temperature during the plasma irradiation for each plasma

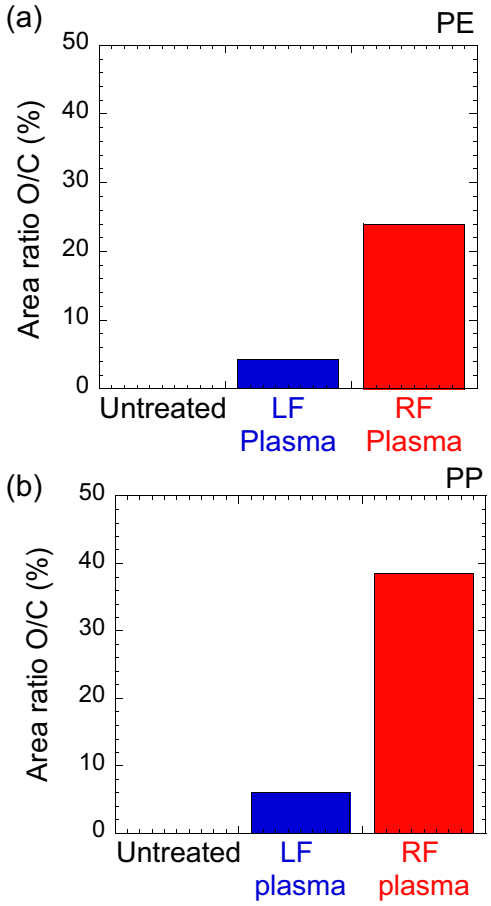

FIGURE 5 | Area ratio between total peak areas of C–O, C=O, and C=O–C bonds and that of C–C bond, calculated from XPS C1s spectra of (a) PE and (b) PP.

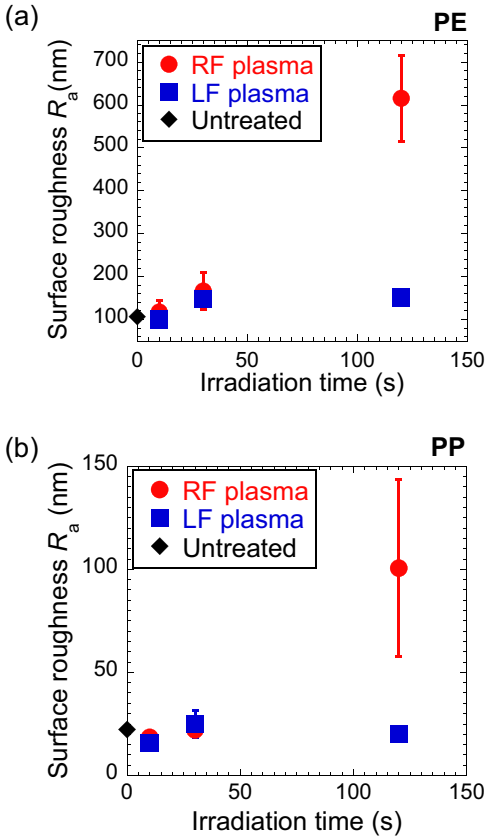

FIGURE 6 | Surface roughness R_a of (a) PE and (b) PP surface as a function of plasma irradiation time.

source. With increasing irradiation time, little change in the surface temperature was observed in the case of LF plasma, but the surface temperature increased from 120°C to 170°C in the case of RF plasma. Compared to LF plasma irradiation, the surface temperature of PP during RF plasma irradiation was found to increase sufficiently with the irradiation time. In previous study, the gas temperature in the RF plasma jet was measured near the head of the glass tube was as high as 140°C. The heat supplied by the plasma results in the heating of the polymer surface [19]. Figure 9 shows the variation in Vickers hardness as a function of the PP surface temperature during both plasma irradiation and heater-induced heating. In all cases, the surface temperatures of PP and PE were measured using an infrared thermometer. In heater heating, the Vickers hardness of the PP surface was observed to decrease under the same thermal conditions as during plasma irradiation. This result indicates that the decline in Vickers hardness resulting from RF plasma irradiation is attributable to thermal degradation.

Polyolefins, including PE and PP, undergo oxidative degradation upon exposure to heat or light in environments containing oxygen and reactive oxidative species. This initiates an auto-oxidation reactions characterized by a chain-reaction mechanism, ultimately leading to the decomposition of the polymer chains into various oxygen-containing functional groups, such as OH, C=O, CHO, COOH, and COOR groups [32–38]. In particular, PP containing tertiary carbon atoms undergoes hydrogen abstraction at these sites, leading to the formation of carbonyl groups as well as hydroperoxides and peroxides. These intermediates subsequently trigger chain reactions that reduce the degree of polymerization (i.e., induce low molecular weight formation) and ultimately cause polymer degradation [39, 40]. Considering the thermal properties of each polymer at their respective temperatures, the glass transition temperatures are approximately −120°C for PE and −20°C for PP. Accordingly, the mechanical performance of polymers is frequently assessed with reference to their melting points; the melting points of PE and PP are 130°C and 160°C, respectively, with PP exhibiting the higher value. The susceptibility of PP to auto-oxidation is known to arise from its intrinsic molecular structure. Such thermally induced structural changes in the polymer are considered to exert minimal influence on its mechanical properties.

From these reactions, the molecular weights of PP decrease, and the resulting polymer embrittlement is thought to be the result of the loss of the hardness of the respective surfaces. Furthermore, although not confirmed by the photograph of the fractured surface shown in Figure 3, the low-molecular-weight and embrittled polymer may have peeled off from the bonded surface, weakening the bond strength.

To control the surface temperature of PP during plasma irradiation using an RF plasma jet, the bonding strength of the epoxy adhesively bonded joints of SPFC980Y bonded to PP was

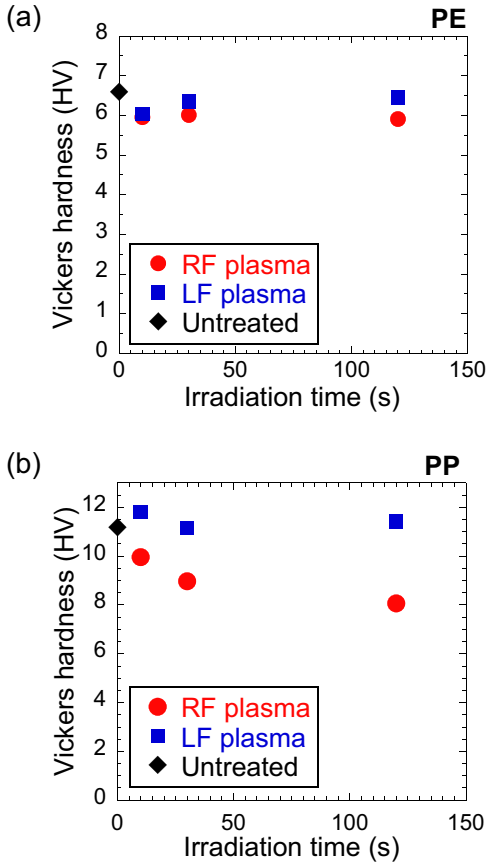

FIGURE 7 | Variation in Vickers hardness of (a) PE and (b) PP surfaces under plasma irradiation as a function of plasma irradiation conditions.

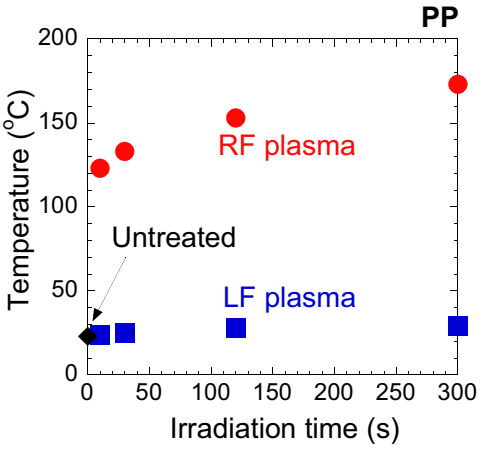

FIGURE 8 | Substrate temperature during plasma irradiation in each plasma source.

evaluated by varying the plasma irradiation distance to PP surface. Figure 10 shows the tensile shear strength of the adhesively bonded joints of SPFC980Y bonded to PP and the surface temperature as a function of the distance from the RF plasma source edge to the PP surface. As the distance from the plasma source to the PP surface increased, the tensile shear strength of the adhesively bonded joint rose to 5 MPa at a distance of 40 mm, after which it declined. In contrast, the surface temperature decreased monotonically from 130°C to 25°C with increasing

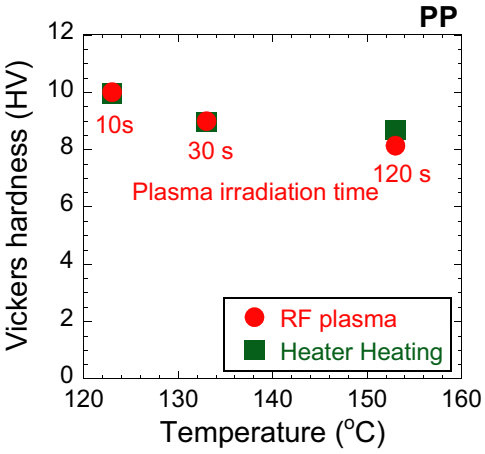

FIGURE 9 | Variation in Vickers hardness on the surface of PP as a function of temperature during plasma irradiation and heater-induced heating.

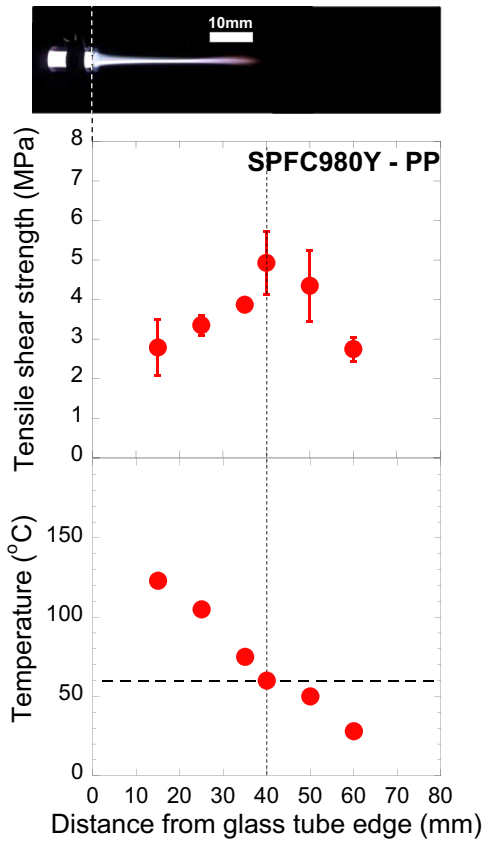

FIGURE 10 | Tensile shear strength of SPFC980Y-PP bonded samples irradiated to RF plasma, surface temperature as a function of distance from the plasma source edge to the PP surface. (RF power: 98 W, Plasma irradiation time 10 s).

distance. The RF plasma source employed in this experiment was designed to extend the plasma plume length up to 40 mm as illustrated in Figure 10. During interaction with the ambient atmosphere, entrainment of surrounding gases into the plasma flow generates oxygen radicals, which are subsequently transported downstream [20]. In previous study, the absolute O atom density within the plasma generated by the atmospheric-pressure

RF plasma jet was measured, revealing that a high oxygen atom density on the order of 10^{14} cm^{-3} is produced near the glass tube head, which was observed to decrease linearly with increasing distance [20]. The PP surface directly exposed to the plasma plume is heated by the thermal energy of the plasma; however, this heating effect diminishes as the distance between the plasma source and the surface increases. According to previous studies on thermal oxidative degradation under oxygen-rich conditions, degradation of PP has been observed to initiate at 63°C under conditions that promote chain scission and oxidative deterioration [41]. As a result, at a plasma-to-surface distance of 40 mm, the tensile shear strength reached its maximum, likely due to the suppression of thermal degradation of PP and the effective surface oxidation induced by oxygen-based reactive species in the plasma. In contrast, when the distance exceeded 40 mm, the oxygen radicals generated within the plasma plume diffused within the gas flow, leading to a reduced flux of oxygen species to the surface. This suppression of surface oxidation resulted in a decline in bonding strength. The results demonstrate that optimizing the RF plasma irradiation conditions can effectively control the radical incident flux and surface temperature impacting the organic material surface. This process provides efficient and appropriate surface treatment at an appropriate temperature range that can flexibly respond to the unique characteristics of organic materials.

4 | Conclusions

Effects of atmospheric-pressure nonequilibrium plasma pretreatment of PE and PP on epoxy adhesively bonded joints have been investigated. The atmospheric-pressure plasma sustained by RF plasma and LF plasma has been used to pretreat PP and PE surfaces. The tensile shear strength of the epoxy adhesively bonded joints of a SPFC980Y bonded to PE and PP pretreated with RF and LF plasma was higher than that of the untreated samples. Conversely, the tensile shear strength for the adhesively bonded joints of a SPFC980Y bonded to PP treated with LF plasma exhibited a higher bonding strength than those treated with RF plasma. The reduced bonding strength observed following RF plasma treatment was attributed to the thermal degradation of PP induced by the heat flux generated by the plasma. In contrast, for PE, the impact of thermal degradation is less pronounced than for PP; thus, the introduction of functional groups via surface treatment is considered to have directly enhanced the bonding strength. Based on these results, tensile shear tests were conducted using the adhesively bonded joints of a SPFC980Y bonded to PP treated with varying distances from the plasma source to control thermal exposure during plasma treatment. The results suggest that adhesion strength can be improved by promoting efficient oxidation of the PP surface while mitigating thermal degradation caused by heat flux from plasma.

Author Contributions

Kosuke Takenaka contributed to all parts of this study: conceptualization, investigation, and writing the manuscript. Ryosuke Koyari and Shunsho Shigemori contributed to collecting and analyzing the data of surface measurement and the joining experiments. Giichiro Uchida contributed to assistance of conceptualization, analyzing of the data from investigation. Yuichi Setsuhara contributed to conceptualization, supervision, and project administration. All authors read and approved of the final manuscript.

Acknowledgments

This study was supported in part by funding from DAIHEN Welding and Joining Research Alliance Laboratories at Joining and Welding Research Institute, Osaka University.

Conflicts of Interest

The authors declare no conflicts of interest.

Data Availability Statement

The data that support the findings of this study are available from the corresponding author upon reasonable request.

References

1. A. Patil, A. Patel, and R. Purohit, "An Overview of Polymeric Materials for Automotive Applications," *Materials Today: Proceedings* 4, no. 2A (2017): 3807–3815, https://doi.org/10.1016/j.matpr.2017.02.278.

2. H. A. Maddah, "Polypropylene as a Promising Plastic: A Review," *American Journal of Polymer Science* 6, no. 1 (2016): 1–11, https://doi.org/10.5923/j.ajps.20160601.01.

3. Q. T. Shubhra, A. Alam, and M. Quaiyyum, "Mechanical Properties of Polypropylene Composites: A Review," *Journal of Thermoplastic Composite Materials* 26, no. 3 (2013): 362–391, https://doi.org/10.1177/0892705711428659.

4. N. C. Paxton, M. C. Allenby, P. M. Lewis, and M. A. Woodruff, "Biomedical Applications of Polyethylene," *European Polymer Journal* 118 (2019): 412–428, https://doi.org/10.1016/j.eurpolymj.2019.05.037.

5. J. Jagur-Grodzinski, "Biomedical Application of Functional Polymers," *Reactive and Functional Polymers* 39, no. 2 (1999): 99–138, https://doi.org/10.1016/S1381-5148(98)00054-6.

6. D. Klee and H. Höcker, "Polymers for Biomedical Applications: Improvement of the Interface Compatibility," in *Biomedical Applications Polymer Blends*, G. C. Eastmond, H. Höcker, and D. Klee, eds., Vol. 149 (Advances in Polymer Science, 2000), https://doi.org/10.1007/3-540-48838-3_1.

7. J. R. Rasmussen, E. R. Stedronsky, and G. M. Whitesides, "Introduction, Modification, and Characterization of Functional Groups on the Surface of Low-Density Polyethylene Film," *Journal of the American Chemical Society* 99, no. 14 (1977): 4736–4745, https://doi.org/10.1021/ja00456a035.

8. R. Alaburdaitė and V. Krylova, "Polypropylene Film Surface Modification for Improving Its Hydrophilicity for Innovative Applications," *Polymer Degradation and Stability* 211 (2023): 110334, https://doi.org/10.1016/j.polymdegradstab.2023.110334.

9. S. W. Ha, R. Hauert, K. H. Ernst, and E. Wintermantel, "Surface Analysis of Chemically-Etched and Plasma-Treated Polyetheretherketone (PEEK) for Biomedical Applications," *Surface and Coatings Technology* 96 (1997): 293–299, https://doi.org/10.1016/S0257-8972(97)00179-5.

10. H. Shi, J. Sinke, and R. Benedictus, "Surface Modification of PEEK by UV Irradiation for Direct Co-Curing With Carbon Fibre Reinforced Epoxy Prepregs," *International Journal of Adhesion and Adhesives* 73 (2017): 51–57, https://doi.org/10.1016/j.ijadhadh.2016.07.017.

11. P. Yang and W. Yang, "Surface Chemoselective Photo Transformation of C–H Bonds on Organic Polymeric Materials and Related High-Tech Applications," *Chemical Reviews* 113 (2013): 5547–5594, https://doi.org/10.1002/chem.201402786.

12. T. Endo, L. Reddy, H. Nishikawa, S. Kaneko, Y. Nakamura, and K. Endo, "Composite Engineering—Direct Bonding of Plastic PET Films by Plasma Irradiation," *Procedia Engineering* 171 (2017): 88–103, https://doi.org/10.1016/j.proeng.2017.01.031.

13. G. D. Davis, "Surface Treatments of Selected Materials," in *Handbook of Adhesion Technology*, L. F. M. da Silva, A. Öchsner, and R. D. Adams Berli, eds. (Springer-Verlag Berlin Heidelberg, 2011).

14. M. Noeske, J. Degenhardt, S. Strudthoff, and U. Lommatzsch, "Plasma Jet Treatment of Five Polymers at Atmospheric Pressure: Surface Modifications and the Relevance for Adhesion," *International Journal of Adhesion and Adhesives* 24 (2004): 171–177, https://doi.org/10.1016/j.ijadhadh.2003.09.006.

15. U. Lommatzsch, D. Pasedag, A. Baalmann, G. Ellinghorst, and H. E. Wagner, "Atmospheric Pressure Plasma Jet Treatment of Polyethylene Surfaces for Adhesion Improvement," supplement, *Plasma Processes and Polymers* 4 (2007): S1041–S1045, https://doi.org/10.1002/ppap.200732402.

16. K. G. Kostov, T. M. C. Nishime, A. H. R. Castro, A. Toth, and L. R. O. Hein, "Surface Modification of Polymeric Materials by Cold Atmospheric Plasma Jet," *Applied Surface Science* 314 (2014): 367–375, https://doi.org/10.1016/j.apsusc.2014.07.009.

17. M. Laroussi and T. Akan, "Arc-Free Atmospheric Pressure Cold Plasma Jets: A Review," *Plasma Processes and Polymers* 4 (2007): 777–788, https://doi.org/10.1002/ppap.200700066.

18. O. J. Kwon, S. W. Myung, C. S. Lee, and H. S. Choi, "Comparison of the Surface Characteristics of Polypropylene Films Treated by Ar and Mixed Gas (Ar/O_2) Atmospheric Pressure Plasma," *Journal of Colloid and Interface Science* 295 (2006): 409–416, https://doi.org/10.1016/j.jcis.2005.11.003.

19. G. Uchida, K. Kawabata, T. Ito, K. Takenaka, and Y. Setsuhara, "Development of a Non-Equilibrium 60 MHz Plasma Jet With a Long Discharge Plume," *Journal of Applied Physics* 122 (2017): 033301, https://doi.org/10.1063/1.4993715.

20. G. Uchida, K. Takenaka, K. Takeda, K. Ishikawa, M. Hori, and Y. Setsuhara, "Selective Production of Reactive Oxygen and Nitrogen Species in the Plasma-Treated Water by Using a Nonthermal High-Frequency Plasma Jet," *Japanese Journal of Applied Physics* 57 (2018): 0102B4, https://doi.org/10.7567/JJAP.57.0102B4.

21. K. Takenaka, R. Machida, T. Bono, et al., "Development of a Non-Thermal Atmospheric Pressure Plasma-Assisted Technology for the Direct Joining of Metals With Dissimilar Materials," *Journal of Manufacturing Processes* 75 (2022): 664–669, https://doi.org/10.1016/j.jmapro.2022.01.041.

22. K. Takenaka, A. Jinda, S. Nakamoto, et al., "Influence of Pre-Treatment Using Non-Thermal Atmospheric Pressure Plasma Jet on Aluminum Alloy A1050 to PEEK Direct Joining With Hot-Pressing Process," *International Journal of Advanced Manufacturing Technology* 130 (2024): 1925–1933, https://doi.org/10.1007/s00170-023-12827-7.

23. K. Takenaka, A. Jinda, S. Nakamoto, et al., "Improving Bonding Strength by Non-Thermal Atmospheric Pressure Plasma-Assisted Technology for A5052/PEEK Direct Joining," *International Journal of Advanced Manufacturing Technology* 130 (2024): 903–913, https://doi.org/10.1007/s00170-023-12747-6.

24. K. Takenaka, S. Nakamoto, R. Koyari, et al., "Influence of Pre-Treatment With Non-Thermal Atmospheric Pressure Plasma on Bond Strength of TP340 Titanium-Peek Direct Bonding," *International Journal of Advanced Manufacturing Technology* 134 (2024): 1637–1644, https://doi.org/10.1007/s00170-024-14160-z.

25. JIS Z 2244, "Vickers Hardness Test—Test Method" (2009).

26. J. Glazer, "Monolayer Studies of Some Ethoxylin Resin Adhesives and Related Compounds," *Journal of Polymer Science* 13, no. 70 (1954): 355–369, https://doi.org/10.1002/pol.1954.1201370117.

27. K. Nakamae, T. Nishino, X. Airu, and S. Asaoka, "Localization of the Curing Agent at an Epoxy Resin/Oxidized Aluminium Interface," *International Journal of Adhesion and Adhesives* 15 (1995): 15–20, https://doi.org/10.1016/0143-7496(95)93638-2.

28. R. Morent, N. De Geyter, C. Leys, L. Gengembre, and E. Payen, "Comparison Between XPS- and FTIR-Analysis of Plasma-Treated Polypropylene Film Surfaces," *Surface and Interface Analysis* 40, no. 3–4 (2008): 597–600, https://doi.org/10.1002/sia.2619.

29. A. Eceiza, M. D. Martin, K. de la Caba, et al., "Thermoplastic Polyurethane Elastomers Based on Polycarbonate Diols With Different Soft Segment Molecular Weight and Chemical Structure: Mechanical and Thermal Properties," *Polymer Engineering & Science* 48 (2008): 297–306, https://doi.org/10.1002/pen.20905.

30. A. Kaji, Y. Arimatsu, and M. Murano, "13C-NMR Study of Anomalous Linkages in Polyurethane," *Journal of Polymer Science, Part A: Polymer Chemistry* 30 (1992): 287–297, https://doi.org/10.1002/pola.1992.080300213.

31. C. Ochoa-Putman and U. K. Vaidya, "Mechanisms of Interfacial Adhesion in Metal–Polymer Composites – Effect of Chemical Treatment," *Composites, Part A: Applied Science and Manufacturing* 42 (2011): 906–915, https://doi.org/10.1016/j.compositesa.2011.03.019.

32. J. L. Bolland and G. Gee, "Kinetic Studies in the Chemistry of Rubber and Related Materials. II. The Kinetics of Oxidation of Unconjugated Olefins," *Transactions of the Faraday Society* 42 (1946): 236–243, https://doi.org/10.1039/TF9464200236.

33. J. L. Bolland, "Kinetic Studies in the Chemistry of Rubber and Related Materials. VI. The Benzoyl Peroxide-Catalysed Oxidation of Ethyl Linoleate," *Transactions of the Faraday Society* 44 (1948): 669–677, https://doi.org/10.1039/TF9484400669.

34. A. B. Mathur and G. N. Mathur, "Thermo-Oxidative Degradation of Isotactic Polypropylene Film: Structural Changes and Its Correlation With Properties," *Polymer* 23 (1982): 54–56, https://doi.org/10.1016/0032-3861(82)90014-3.

35. P. Gijsman and R. Fiorio, "Long Term Thermo-Oxidative Degradation and Stabilization of Polypropylene (PP) and the Implications for Its Recyclability," *Polymer Degradation and Stability* 208 (2023): 110260, https://doi.org/10.1016/j.polymdegradstab.2023.110260.

36. A. Hoff and S. Jacobsson, "Thermo-Oxidative Degradation of Low-Density Polyethylene Close to Industrial Processing Conditions," *Journal of Applied Polymer Science* 26 (1981): 3409–3423, https://doi.org/10.1002/app.1981.070261020.

37. M. Da Cruz, L. Van Schoors, K. Benzarti, and X. Colin, "Thermo-Oxidative Degradation of Additive Free Polyethylene. Part I. Analysis of Chemical Modifications at Molecular and Macromolecular Scales," *Journal of Applied Polymer Science* 133 (2016): 43287, https://doi.org/10.1002/app.43287.

38. T. Shahsavari-Badvestani, R. Jahanmardi, M. I. Tayouri, and M. Fathi, "Acceleration of Thermo-Oxidative Degradation of High-Density Polyethylene Using Oxidized Polyethylene," *Polymer Journal* 10 (2023): 149–157, https://doi.org/10.22063/poj.2023.3288.1246.

39. D. M. Mowery, R. A. Assink, D. K. Derzon, S. B. Klamo, R. L. Clough, and R. Bernstein, "Solid-State 13C NMR Investigation of the Oxidative Degradation of Selectively Labeled Polypropylene by Thermal Aging and γ-Irradiation," *Macromolecules* 38, no. 12 (2005): 5035–5046, https://doi.org/10.1021/ma047381b.

40. R. S. G. Romano, W. L. Oliani, D. F. Parra, and A. B. Lugao, "Accelerated Environmental Degradation of Gamma Irradiated Polypropylene and Thermal Analysis," *Journal of Thermal Analysis and Calorimetry* 131 (2018): 823–828, https://doi.org/10.1007/s10973-017-6653-1.

41. T. Iizuka, Y. Ohtake, and K. Tanaka, "A Synergistic Effect of Light and Heat on Degradation for Polypropylene," *Journal of the Society of Materials Science, Japan* 66 (2017): 238–243, https://doi.org/10.2472/jsms.66.238.